Research Square

Preprints are preliminary reports that have not undergone peer review.
They should not be considered conclusive, used to inform clinical practice,
or referenced by the media as validated information.

Normal-state exponential muon-spin relaxation and its implications for time-reversal symmetry breaking in Sr$_2$RuO$_4$

Rustem Khasanov

rustem.khasanov@psi.ch

PSI Center for Neutron and Muon Sciences CNM https://orcid.org/0000-0002-4768-5524

Thomas Hicken

PSI Center for Neutron and Muon Sciences CNM https://orcid.org/0000-0003-4812-0426

Jonas Krieger

Paul Scherrer Institute https://orcid.org/0000-0003-3337-5530

Maxime Lamotte

PSI Center for Neutron and Muon Sciences CNM

Toni Shiroka

Laboratory for Muon Spin Spectroscopy, Paul Scherrer Institute

Jake Bobowski

University of British Columbia https://orcid.org/0000-0001-6769-0438

Vadim Grinenko

Tsung-Dao Lee Institute, Shanghai Jiao Tong University

Thomas Johnson

Department of Engineering, Kyoto University of Advanced Science

Naoki Kikugawa

National Institute for Materials Science https://orcid.org/0000-0003-3975-4478

Hans-Henning Klauss

Institute of Solid State and Materials Physics, Technical University Dresden https://orcid.org/0000-0002-8523-0491

Paul Shubhankar

Department of Physics, Indian Institute of Technology Kanpur https://orcid.org/0009-0004-0587-0336

Benjamin Huddart

University of Oxford https://orcid.org/0000-0001-8584-105X

Stephen Blundell

University of Oxford https://orcid.org/0000-0002-3426-0834

Hubertus Luetkens

Paul Scherrer Institute https://orcid.org/0000-0002-5842-9788

Yoshiteru Maeno
Toyota Riken-Kyoto University Research Center (TRiKUC), Kyoto University https://orcid.org/0000-0002-3467-9416

Article

Keywords:

Posted Date: November 20th, 2026

DOI: https://doi.org/10.21203/rs.3.rs-11447024/v1

License: This work is licensed under a Creative Commons Attribution 4.0 International License.
Read Full License

Additional Declarations: There is **NO** Competing Interest.

Normal-state exponential muon-spin relaxation and its implications for time-reversal symmetry breaking in Sr_2RuO_4

Rustem Khasanov,[1,*] Thomas J. Hicken,[1] Jonas A. Krieger,[1] Maxime Lamotte,[1] Toni Shiroka,[1] Jake S. Bobowski,[2,3] Vadim Grinenko,[4] Thomas Johnson,[5,3] Naoki Kikugawa,[6] Hans-Henning Klauss,[7] Shubhankar Paul,[8,3] Benjamin M. Huddart,[9] Stephen J. Blundell,[9] Hubertus Luetkens,[1] and Yoshiteru Maeno[5,3,10,†]

[1] *PSI Center for Neutron and Muon Sciences, 5232 Villigen PSI, Switzerland*
[2] *Department of Physics, University of British Columbia, Kelowna, BC V1V 1V7, Canada*
[3] *Toyota Riken - Kyoto-Univ. Research Center (TRiKUC), Kyoto 606-8501, Japan*
[4] *Tsung-Dao Lee Institute & School of Physics and Astronomy, Shanghai Jiao Tong University, Shanghai 201210, China*
[5] *Department of Engineering, Kyoto University of Advanced Science (KUAS), Kyoto 615-8577, Japan*
[6] *National Institute for Materials Science, Tsukuba 305-0003, Japan*
[7] *Institut für Festkörper und Materialphysik, Technische Universität Dresden, 01062 Dresden, Germany*
[8] *Department of Physics, Indian Institute of Technology Kanpur, Kanpur 208016, India*
[9] *Clarendon Laboratory, University of Oxford, Department of Physics, Oxford OX1 3PU, United Kingdom*
[10] *Max Planck Institute for Chemical Physics of Solids (MPI-CPfS), Nöthnitzer Str. 40, 01187 Dresden, Germany*

(Dated: November 13, 2026)

Abstract.
The low-temperature increase of the zero-field muon-spin relaxation rate in Sr_2RuO_4 has long been regarded as evidence for spontaneous internal fields associated with time-reversal-symmetry-breaking (TRSB) superconductivity. Here we directly test this interpretation using muon-spin rotation/relaxation (μSR) measurements on high-quality Sr_2RuO_4 single crystals. For all four samples, the onset temperature of the additional exponential relaxation in the zero-field μSR data, T_Λ, lies below the bulk superconducting transition temperature T_c, even in the absence of applied strain. More importantly, in transverse-field μSR measurements we find a quantitatively similar exponential relaxation in a field of 80 mT applied along the crystallographic c axis. This field exceeds the upper critical field of the crystals studied in transverse-field geometry and suppresses bulk superconductivity, demonstrating that the characteristic relaxation persists in the normal state. Measurements below the upper critical field reveal an additional superconducting mixed-state contribution superposed on this normal-state channel. Our results show that the zero-field μSR relaxation in Sr_2RuO_4 cannot, by itself, be regarded as a unique signature of superconducting TRSB. They call for a reassessment of a key experimental signature of TRSB in Sr_2RuO_4 and highlight the need to distinguish superconducting and normal-state relaxation channels in other unconventional superconductors.

I. INTRODUCTION

Sr_2RuO_4, despite its modest superconducting transition temperature T_c of about 1.5 K, remains a central material in the study of unconventional superconductivity. Its normal-state electronic structure is exceptionally well characterized, but the superconducting order parameter is still debated three decades after the discovery of superconductivity [1–4]. Early experiments were interpreted as supporting a spin-triplet chiral p-wave state. In particular, early ^{17}O nuclear magnetic resonance (NMR) Knight-shift measurements suggested an unchanged spin susceptibility below T_c [5], while zero-field muon-spin rotation/relaxation (ZF-μSR) experiments detected an enhanced relaxation below T_c, interpreted as the appearance of spontaneous internal fields due to time-reversal symmetry breaking (TRSB) [6, 7]. Polar Kerr measurements also detected a finite Kerr angle below T_c [8], and Josephson experiments were interpreted in terms of a complex order parameter [9, 10].

The original chiral p-wave scenario has, however, become difficult to reconcile with later experiments. Revised NMR Knight-shift measurements showed a decrease of the spin susceptibility below T_c [11–13], and polarized neutron scattering reached a compatible conclusion [14]. A recent high-precision muon Knight-shift experiment also found a reduction of the Knight shift below T_c, providing an independent μSR constraint consistent with spin-singlet-like pairing [15]. The present debate has therefore shifted toward even-parity order parameters. If TRSB is intrinsic to the superconducting state, possible candidates include complex combinations such as $d_{xz} \pm id_{yz}$, $s \pm id$, or $d \pm ig$ [16, 17]. These states generally imply either a symmetry-protected two-component order parameter or an accidental near-degeneracy of two one-dimensional representations [16–18]. A distinct possibility is inhomogeneous TRSB near defects or dislocations in an otherwise time-reversal symmetric single-component superconducting state [19].

Several recent thermodynamic and strain experiments have sharpened this problem. Ultrasound experiments reported jumps in the shear elastic modulus c_{66} at T_c, which can be interpreted as evidence for a multicompo-

* rustem.khasanov@psi.ch
† maeno.yoshiteru.b04@kyoto-u.jp

nent order parameter [20, 21]. For such a state, uniaxial strain is expected to lift the degeneracy between the components and, in general, to split the superconducting and TRSB transitions. A split between T_c and T_{TRSB} was indeed reported by μSR under uniaxial stress [22, 23]. However, this behavior has not been confirmed by thermodynamic probes: high-sensitivity heat-capacity measurements under uniaxial pressure found no evidence for a second transition [24]. Elastocaloric measurements under uniaxial strain further mapped the thermodynamic phase diagram of Sr_2RuO_4, including the superconducting phase boundary and a strain-induced magnetic phase [25]. More recently, high-resolution measurements of T_c and the elastocaloric effect under $\langle 110 \rangle$ uniaxial stress found no indication of the transition splitting expected for a homogeneous two-component TRSB superconducting state [26]. Thus, the strain-induced split between T_c and the putative TRSB onset is presently a μSR-specific observation. This discrepancy raises the question of whether the onset of ZF-μSR relaxation indicates a bulk superconducting transition. This question is particularly important for unstrained Sr_2RuO_4, where tetragonal symmetry is preserved and a homogeneous intrinsic TRSB superconducting state would be expected to have $T_{TRSB} = T_c$.

To address this question, we compare the available zero-field μSR results on unstrained Sr_2RuO_4 from Refs. [6, 7, 16, 22, 23, 27–30]. The comparison is shown in Fig. 1, where the bulk superconducting transition temperature T_c is plotted against the onset temperature T_Λ extracted from the exponential ZF-μSR relaxation rate Λ. To place the literature data on the same footing, the temperature dependence of the exponential relaxation rate was fitted, where possible, with the phenomenological form used in Refs. [16, 22]:

$$\Lambda(T) = \begin{cases} \Lambda_0, & T > T_\Lambda, \\ \Lambda_0 + \Delta\Lambda \left[1 - (T/T_\Lambda)^n\right], & T < T_\Lambda, \end{cases} \quad (1)$$

where Λ_0 is the high-temperature relaxation rate, $\Delta\Lambda$ is the low-temperature enhancement, and n is a phenomenological power-law exponent. Although many points lie close to $T_\Lambda = T_c$ (the dashed line in Fig. 1), a substantial fraction of the ZF-μSR data show $T_\Lambda < T_c$. This spread indicates a nonuniversal relation between the exponential relaxation and superconductivity. If T_Λ were the onset of a homogeneous TRSB superconducting state, one would expect a robust bulk transition and, when separated from T_c, a corresponding anomaly in other probes.

In this paper we revisit the μSR evidence from a different perspective. We study four unstrained Sr_2RuO_4 single crystals with different T_c values. We compare zero-field (ZF) relaxation with transverse-field (TF) relaxation measured at fields both below and above the upper critical field for $H \parallel c$ ($H_{c2}^{\parallel c}$). Since the zero-temperature upper critical field $\mu_0 H_{c2}^{\parallel c}(0)$ is below 80 mT for all studied crystals, the 80 mT TF-μSR data provide an empirical measure of relaxation processes present

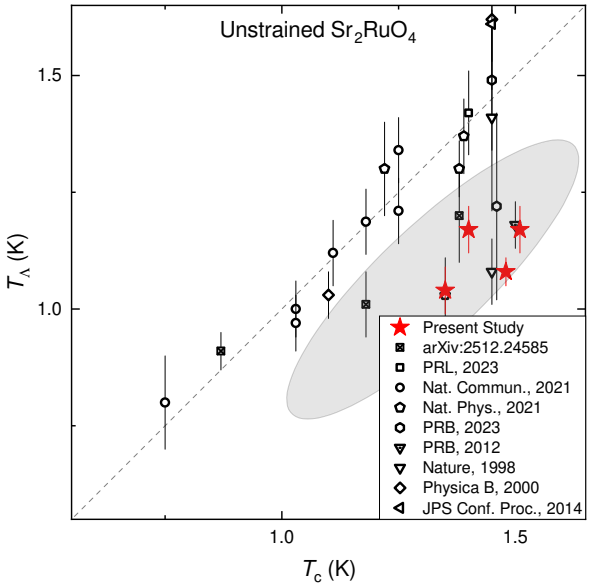


FIG. 1. Comparison between the bulk superconducting transition temperature T_c and the onset temperature T_Λ of the exponential relaxation rate Λ for unstrained Sr_2RuO_4. Red stars denote the present samples. Open and partly filled symbols summarize data from previous ZF-μSR studies, including Refs. [6, 7, 16, 22, 23, 27–30]. The dashed line corresponds to $T_\Lambda = T_c$. The gray region highlights the samples showing the strongest separation between T_c and T_Λ.

when bulk superconductivity is suppressed. We also use muon stopping-site calculations and simulations of the nuclear contribution to assess whether static nuclear moments can account for the observed ZF relaxation.

We find that the low-temperature exponential relaxation observed in ZF-μSR has a close counterpart in this normal-state data set. By contrast, TF-μSR measurements below $H_{c2}^{\parallel c}(0)$ reveal an additional relaxation associated with the vortex state, superposed on the same underlying normal-state relaxation channel. This approach allows us to separate superconductivity-related broadening from relaxation processes that are already present in the normal state, and provides a direct test of whether the ZF-μSR relaxation anomaly is a universal signature of bulk TRSB in Sr_2RuO_4.

II. EXPERIMENTAL DETAILS

The μSR experiments were performed on four Sr_2RuO_4 single crystals, denoted here as samples A–D. The corresponding original sample labels are A (C516E2R), B (C507BC), C (C501C), and D (C140). All samples were grown at Kyoto University [31]. Details of the crystal-growth procedure, photographs of the crystals, and Laue x-ray images are provided in the Supplementary Information. The samples used in the present study are of high quality, as confirmed by their sharp superconducting transitions and by the small amount of impurity phases

detected in dc-magnetization measurements performed at 10 mT and 1 T; see the Supplementary Information.

The superconducting properties of samples A–C were characterized by ac susceptibility, as described in the Supplementary Information. The superconducting transition temperatures were determined from the peak position of the imaginary part of the ac-susceptibility signal and were found to be T_c=1.51(1), 1.48(1), and 1.40(1) K for samples A, B, and C, respectively. For sample D, the superconducting transition temperature was determined from specific-heat measurements and reported to be T_c=1.35(2) K [16].

The main set of zero-field (ZF), transverse-field (TF), and longitudinal-field (LF) μSR experiments was performed on samples A–C. For sample D, only ZF-μSR measurements were performed. Most of the μSR experiments were carried out on the FLAME μSR spectrometer at the Paul Scherrer Institute (PSI, Villigen, Switzerland), using a dilution refrigerator. These measurements were performed in ZF and in applied fields up to 1 T, over the temperature range from 40 mK to 2 K. The accessible temperature interval was set by the weak-thermal-link mode of operation, which allows the temperature to be scanned over this range without losing the ^{3}He–^{4}He mixture. To exclude possible spectrometer- or cryostat-related effects, the ZF-μSR measurements on sample B were repeated on the VMS μSR spectrometer, also at PSI, using a ^{3}He sorption-pump cryostat with a base temperature of 0.25 K. The data were analyzed using the MUSRFIT package [32].

The experimental geometry and data-analysis procedure are discussed in the Supplementary Information. The exponential relaxation rates obtained from fits of the ZF-, TF-, and LF-μSR data, which are the main focus of this paper, are denoted by Λ^{ZF}, Λ^{TF}, and Λ^{LF}, respectively.

Use of AI tools. Anthropic's Claude Opus 5 was used to write the analysis and plotting scripts that generate the tabulated coordinates, barriers, and zero-point energies, as well as Fig. 7 and Figs. S13–S15 in the Supplementary Information; to assist with preparing, running, and analyzing the calculations; to help identify relevant literature; and to edit the text. Claude Fable 5.1 was used to help formulate the symmetry arguments used to identify candidate transition states. All arguments, calculations, and outputs were checked by the authors, who take full responsibility for the content.

III. RESULTS

A. Upper critical field

Before comparing the ZF- and TF-μSR relaxation rates, it is necessary to establish the field-temperature boundary between the superconducting and normal states. The $T_c(H)$ points for samples A–C were determined from zero-field-cooled (ZFC) and field-cooled (FC) TF-μSR measurements with $H \parallel c$. At each applied field, the transition temperature was identified from the onset of the additional Gaussian relaxation σ^{TF} and from the corresponding change in the internal field B_{int}, as demonstrated for samples A–C in the Supplementary Information.

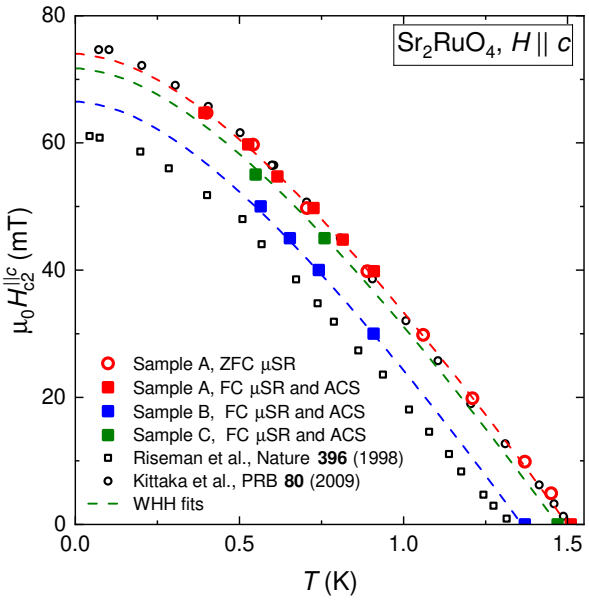


FIG. 2. The temperature dependence of the upper critical field $H_{c2}^{\|c}$ in $H \parallel c$ for samples A–C. Literature data from Riseman *et al.* [33] and Kittaka *et al.* [34] are shown for comparison. Dashed curves are fits based on the Werthamer-Helfand-Hohenberg (WHH) form [35].

The resulting $H_{c2}^{\|c}(T)$ data are summarized in Fig. 2. For comparison, we also show the most complete literature data sets for Sr_2RuO_4 crystals with T_c = 1.28 K and 1.50 K from Refs. 33 and 34. The zero-field transition temperatures of the present samples are either close to the higher-T_c reference crystal, as for sample A with T_c=1.51 K, or lie between the two reference data sets, as for samples B and C with T_c=1.48 and 1.40 K, respectively. The agreement with these literature $H_{c2}^{\|c}(T)$ curves, together with the independently determined zero-field transition temperatures from ac susceptibility, shows that the transitions identified by TF-μSR correspond to the bulk superconducting transition.

The dashed lines in Fig. 2 are fits based on the Werthamer-Helfand-Hohenberg (WHH) form [35]. In performing these fits, we also take into account the scaling reported in Ref. 30, namely that $H_{c2}^{\|c}(T)$ curves for samples with different T_c values collapse approximately onto a common curve when normalized by the zero-field superconducting transition temperature. The fits yield $\mu_0 H_{c2}^{\|c}(0)$ values of 74.0(1), 71.7(1), and 66.5(1) mT for samples A, B, and C, respectively (see also Table I). Thus, for $H \parallel c$, fields exceeding approximately 75 mT suppress bulk superconductivity in the present crystals

down to the lowest temperatures.

TABLE I. Summary of the superconducting transition temperatures, T_c, upper critical fields, $H_{c2}^{\|c}(0)$, and characteristic onset temperatures of the exponential relaxation, T_Λ^{ZF} and $T_\Lambda^{TF,80mT}$, for samples A–D.

Sample	T_c (K)	$\mu_0 H_{c2}^{\|c}(0)$ (mT)	T_Λ^{ZF} (K)	$T_\Lambda^{TF,80mT}$ (K)
A	1.51(1)	74.0(1)	1.14(6)	1.15(7)
B	1.48(1)	71.7(1)	1.04(6)	1.06(7)
C	1.40(1)	66.5(1)	1.14(6)	1.07(6)
D	1.35(2)	–	1.13(5)	–

B. Comparison of zero-field and 80 mT relaxation

The central result of this work is summarized in Fig. 3, where the exponential relaxation rates measured in ZF and in TF at 80 mT are compared directly for samples A–C. The importance of the 80 mT data is that this field exceeds $H_{c2}^{\|c}(0)$ for all three samples, see Table I and Fig. 2. Therefore, the samples are in the normal state, and any relaxation observed at this field cannot originate from the superconducting mixed state or from spontaneous fields associated with a homogeneous superconducting TRSB phase.

Several important points follow from the comparison of ZF and TF 80 mT data:

- The ZF exponential relaxation rate Λ^{ZF} starts to increase only below a temperature T_Λ, which is lower than the bulk superconducting transition temperature T_c. Such behavior is observed for samples A–C in Fig. 3, and also for sample D, as shown in the Supplementary Information. A possible spectrometer- or cryostat-related origin of this effect was ruled out by repeating the ZF-μSR measurements on sample B at the VMS instrument, see the Supplementary Information.

- A very similar temperature dependence is observed for the exponential relaxation rate measured in TF at 80 mT. The increase of Λ^{TF} starts at nearly the same temperature as the increase of Λ^{ZF}, even though bulk superconductivity is completely suppressed at this field.

- Fits of Eq. (1) to $\Lambda^{ZF}(T)$ and $\Lambda^{TF}(T)$ yield closely similar onset temperatures in the two geometries, see Table I and Fig. 3. Note that to reduce correlations between fitting parameters, the final analysis used a common phenomenological exponent fixed at $n = 2.5$, consistent with preliminary fits in which n was allowed to vary independently; see the Supplementary Information.

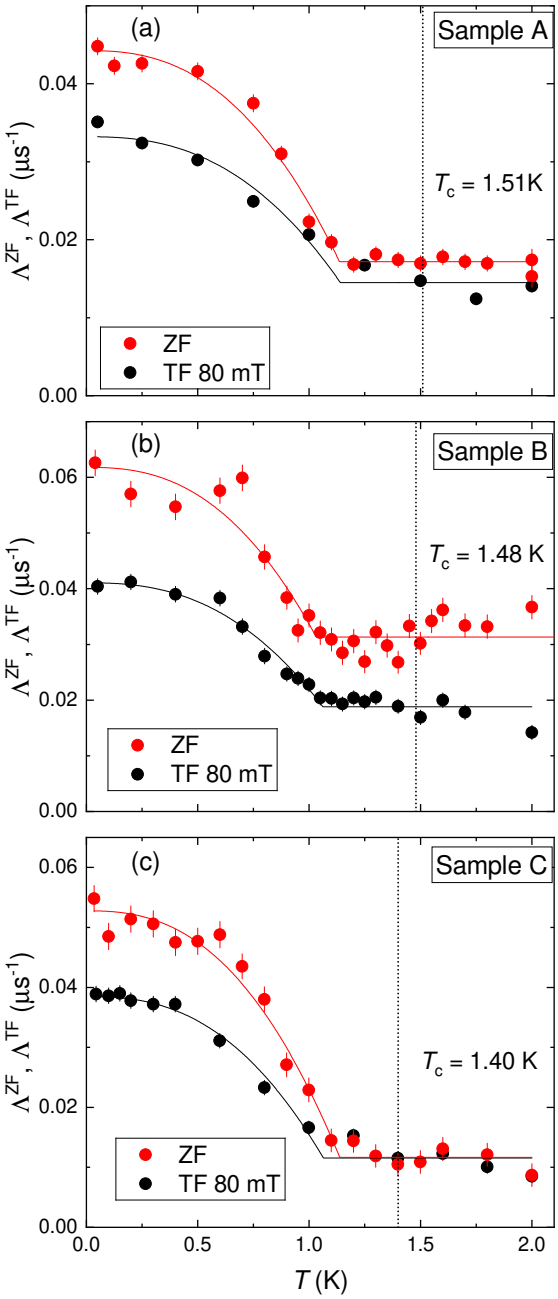


FIG. 3. Temperature dependence of the exponential relaxation rate Λ obtained from ZF- and 80 mT TF-μSR measurements for (a) sample A, (b) sample B, and (c) sample C. The vertical dotted lines mark the bulk superconducting transition temperatures. Solid curves are fits to Eq. (1).

- The absolute increase of the exponential relaxation, $\Delta\Lambda$, is larger in ZF than in TF at 80 mT. However, the ratio

$$\Delta\Lambda^{ZF}/\Delta\Lambda^{TF,80mT} \simeq 1.4\text{–}1.5$$

is approximately the same for all three samples.

- Above T_Λ, the exponential relaxation rate remains finite in both ZF and 80 mT TF measurements. In

ZF, $\Lambda^{\mathrm{ZF}}(T)$ is nearly temperature independent in this range, whereas in TF, $\Lambda^{\mathrm{TF,80mT}}(T)$ shows a weak but systematic decrease with increasing temperature above T_Λ. The presence of this finite relaxation above the apparent onset temperature indicates that the underlying relaxation channel is already present in the normal state. The increase below T_Λ therefore reflects an enhancement or slowing down of a pre-existing channel, rather than the sudden appearance of a completely new contribution.

- When the extracted T_Λ values are plotted as a function of T_c in Fig. 1, the present data follow the tendency observed for several other Sr_2RuO_4 samples, namely that T_Λ remains separated from T_c.

Overall, the close correspondence between the ZF and 80 mT TF relaxation rates shows that a substantial part of the exponential relaxation cannot be assigned uniquely to spontaneous superconducting fields. Instead, the data indicate that the low-temperature increase of Λ originates from a normal-state relaxation mechanism that persists when superconductivity is suppressed.

C. Exponential relaxation in the superconducting and normal states

Figure 4 shows the temperature dependence of $\Lambda^{\mathrm{TF}}(T)$ obtained in TF-μSR measurements performed on samples A–C in fields below $H_{c2}^{\parallel c}(0)$, together with the 80 mT data for comparison. In fields below $H_{c2}^{\parallel c}(0)$, superconductivity is clearly detected by μSR: on cooling through the field-dependent superconducting transition, the internal field decreases and the Gaussian relaxation rate increases, as expected from the formation of a flux-line lattice (see Fig. S9 in the Supplementary Information). The corresponding $T_c(H)$ values are indicated by colored arrows in Fig. 4. The exponential relaxation rate starts to increase already above $T_c(H)$, reflecting the underlying normal-state relaxation channel discussed above. On further cooling through $T_c(H)$, a much stronger additional increase develops in fields below $H_{c2}^{\parallel c}(0)$. Because this additional contribution is observed only below the upper critical field and follows closely the field-dependent superconducting transition, it should be regarded primarily as a superconducting mixed-state contribution.

The comparison with the 80 mT data is important for separating this mixed-state superconducting contribution from the normal-state relaxation channel discussed above. At 80 mT, bulk superconductivity is suppressed in all three samples, yet a weaker and more gradual low-temperature exponential relaxation remains visible. Therefore, the exponential relaxation measured below $H_{c2}^{\parallel c}(0)$ should be regarded as a superposition of two terms: a superconducting vortex contribution and an underlying normal-state exponential channel. For each sample, the 80 mT data provide an empirical estimate of this normal-state channel. In the lower-field TF data, the weak underlying relaxation starts to increase at approximately the same temperature as in the 80 mT data,

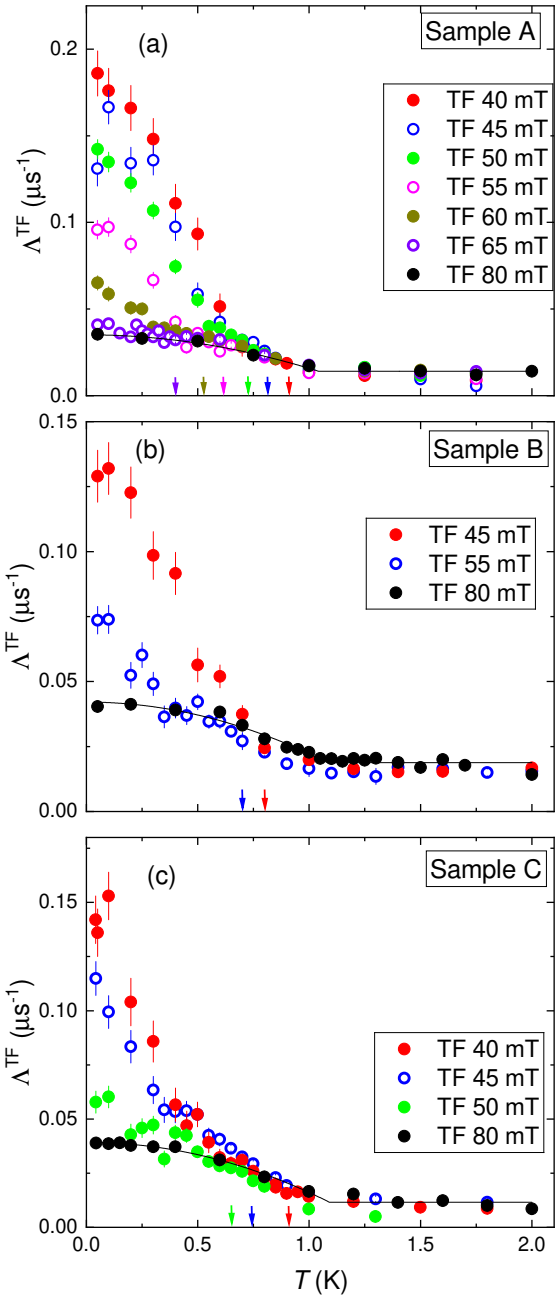


FIG. 4. Exponential relaxation rate obtained in TF-μSR experiments below and above $H_{c2}^{\parallel c}(0)$ for (a) sample A, (b) sample B, and (c) sample C. The large low-temperature relaxation in fields below $H_{c2}^{\parallel c}(0)$ is attributed primarily to the superconducting mixed state. The solid lines are fits of Eq. (1) to the 80 mT TF data. The arrows indicate the superconducting transition temperature T_c determined from the temperature dependences of the Gaussian relaxation rate σ^{TF} and the internal field B_{int}; see the Supplementary Information.

namely near $T_\Lambda^{\mathrm{TF,80mT}}$, within the experimental uncertainty.

To further characterize this normal-state channel, we measured the temperature dependence of the exponential relaxation in constant transverse fields exceeding $H_{c2}^{\parallel c}(0)$. The results are summarized in Fig. 5. For sample A, measurements were performed at 80, 200, 500 mT, and 1 T. The data show that the characteristic temperature scale associated with the change of $\Lambda(T)$ tends to increase with increasing applied field. At 80 and 200 mT, the increase of Λ^{TF} on cooling occurs within the measured temperature range. At 500 mT, the onset is shifted to temperatures above about 2 K, so that only the low-temperature part of the relaxation enhancement is observed. At 1 T, $\Lambda^{\mathrm{TF}}(T)$ changes only weakly over the accessible temperature window, consistent with the characteristic onset being shifted beyond the measured range. The data for sample B show an analogous comparison between 80 and 200 mT, with the higher-field data exhibiting a broader and higher-temperature evolution of $\Lambda^{\mathrm{TF}}(T)$.

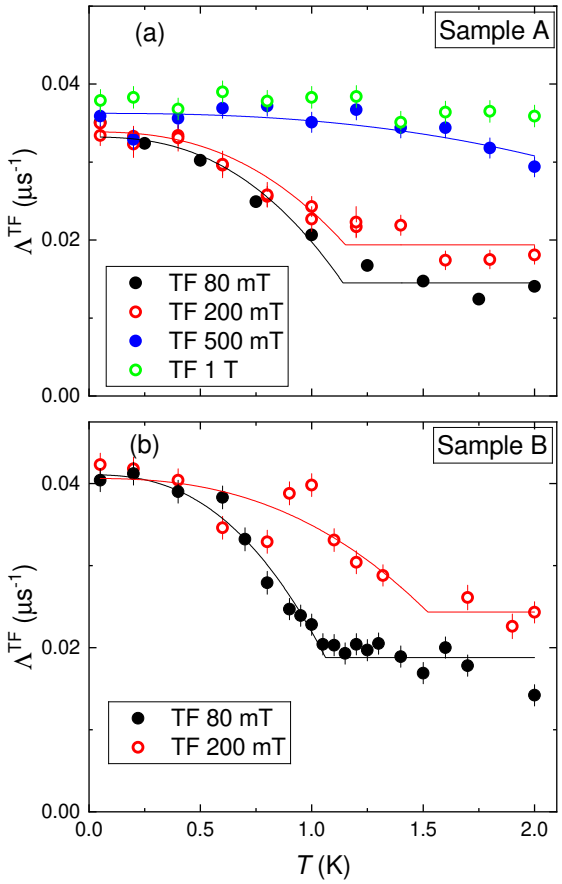


FIG. 5. Temperature dependence of the exponential relaxation rate in transverse-field measurements above $H_{c2}^{\parallel c}(0)$ for (a) sample A and (b) sample B. The solid lines are fits of Eq. (1) to the data.

D. Longitudinal-field μSR experiments

LF-μSR measurements were performed to determine whether the internal fields responsible for the exponential relaxation are static/quasistatic or dynamic on the μSR time scale. In a conventional LF geometry, a longitudinal field applied parallel to the initial muon-spin polarization decouples the muon spins from a static or quasistatic distribution of local fields, whereas relaxation caused by fast fluctuations is not suppressed in the same way [36, 37].

The most complete LF-μSR data set was obtained for sample B, for which the applied longitudinal field was varied from 0.075 to 200 mT. For samples A and C, LF-μSR measurements were performed over more limited field intervals, from 5 mT to 1 T for sample A and from 40 to 80 mT for sample C.

The field dependence of Λ^{LF} for sample B is shown in Fig. 6. The most direct information is obtained at $T = 2$ K, i.e., above the superconducting transition temperature of sample B, T_c=1.48 K. In this normal-state data set, Fig. 6(b), the relaxation is strongly reduced already by longitudinal fields of order 1 mT and is nearly suppressed at higher fields. Such behavior is characteristic of decoupling from a static or quasistatic distribution of local magnetic fields. It disfavors a purely fast-fluctuating origin of the exponential relaxation and instead points to slowly fluctuating or static dilute magnetic fields, or to a temperature-dependent change of the static field distribution sampled by the muons.

The LF data below T_c, shown in Fig. 6(a), require additional care. In a nonsuperconducting sample, a longitudinal field applied parallel to the initial muon-spin polarization decouples static transverse local fields in a relatively direct way. In the superconducting state, however, the internal magnetic field in a real sample is generally not uniform. Partial diamagnetism, demagnetization effects, vortex penetration, and geometrical barriers can all distort the field distribution. Among these effects, the geometrical barrier is expected to be particularly relevant for the present platelet-like crystals. Such a barrier is absent only for ideal ellipsoidal samples, for which the demagnetizing field is homogeneous. In nonellipsoidal samples, by contrast, it affects flux entry and can produce a strongly inhomogeneous spatial distribution of vortices and internal fields [38–42].

The inset of Fig. 6(a), adapted from Brandt [38], illustrates this effect for a rectangular superconducting sample. The field lines are distorted by the geometrical barrier: far from the sample they follow the applied field direction, whereas near the sample edges they bend strongly. Consequently, muons stopping near regions with strong field curvature can experience local fields that are not parallel to the applied LF field. This effect should be less pronounced in large and thin single crystals, where the relative weight of the edge regions is reduced, but it remains an important complication for finite rectangular samples.

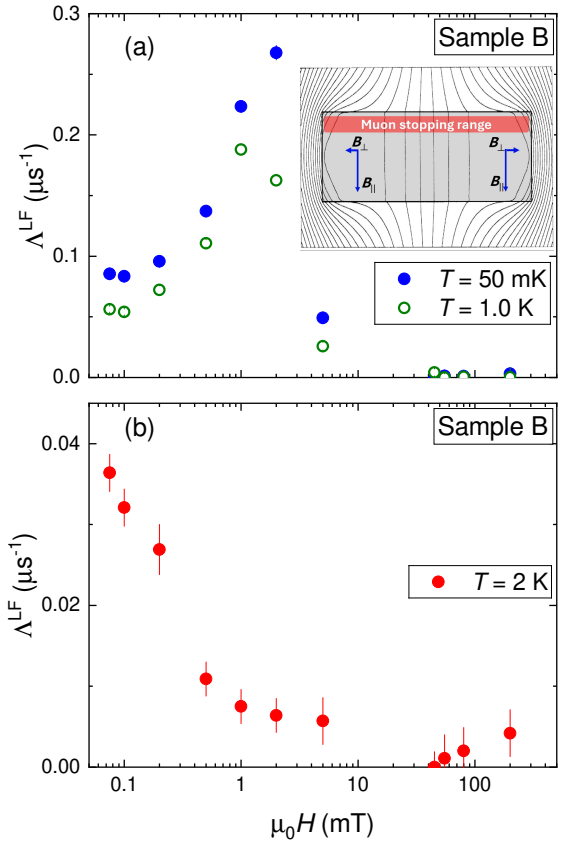


FIG. 6. Longitudinal-field dependence of the exponential relaxation rate Λ^{LF} for sample B at (a) 50 mK and 1.0 K, and (b) 2.0 K. The inset in panel (a), adapted from Brandt [38], schematically illustrates the field distribution in a rectangular superconducting sample affected by partial diamagnetism and a geometrical barrier. Field bending near the sample edges can generate local components perpendicular to the nominal LF direction and can therefore contribute to the LF relaxation.

To summarize, the normal-state LF-μSR measurements provide strong evidence that the exponential relaxation originates from static or quasistatic local fields. In the superconducting state, the LF response is compatible with this conclusion, but a quantitative separation of microscopic magnetism from superconductivity-induced field inhomogeneity requires caution because geometrical barriers and vortex-field distortions can themselves generate transverse local-field components in a nominal LF experiment.

IV. DISCUSSION

In this section, we first summarize the results of the muon stopping-site calculations and estimate the ZF relaxation expected from the nuclear moments of naturally abundant O, Sr and Ru isotopes. We then discuss possible mechanisms that may account for the observed temperature and field evolution of the low-temperature exponential relaxation. Finally, we consider the consequences of our experimental findings for the interpretation of time-reversal-symmetry breaking in Sr_2RuO_4.

A. Muon stopping sites and nuclear contribution to the ZF relaxation

1. *Muon stopping sites and hopping*

To determine the muon stopping sites, we carried out density-functional theory (DFT) calculations using the plane-wave basis-set electronic-structure code CASTEP [43]. Muon-site calculations were performed using the MuFinder program [44]. We confirm the results proposed in Ref. [45], namely that the muon stops approximately 0.97 Å from an apical oxygen of a RuO_6 octahedron.

Among five possible hopping paths connecting symmetry-equivalent muon sites separated by less than 3.0 Å, the shortest path, with a site-to-site distance of 1.25 Å, has the lowest barrier, $V_0 \simeq 70$ meV. This barrier becomes effectively zero once the zero-point energies of the muon at the stopping site and at the top of the barrier are taken into account. By contrast, paths connecting sites associated with different apical oxygen atoms have an effective barrier of approximately 0.37 eV, making long-range muon diffusion negligible at the temperatures of our measurements. The muon should therefore be considered as delocalized over four symmetry-equivalent sites around an apical oxygen; see Fig. 7. Further details of the calculations, including the candidate muon hopping paths, transition states, and zero-point-energy-corrected barriers, are given in the Supplementary Information.

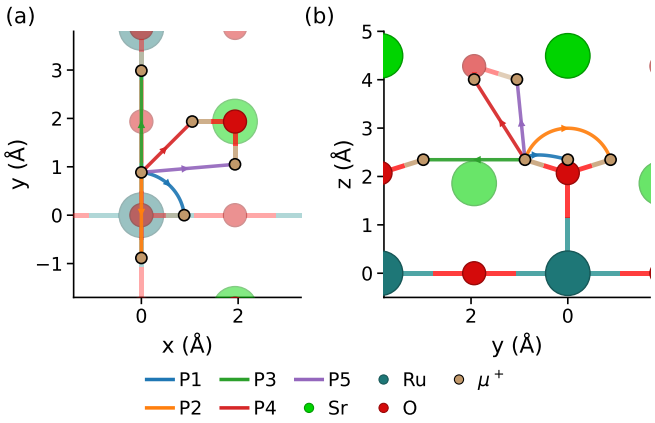


FIG. 7. Candidate muon hopping paths in Sr_2RuO_4, viewed (a) along the c axis and (b) along the a axis. The paths connect symmetry-equivalent copies of the lowest-energy muon site. Atomic layers further away from the viewer are shown with increasing transparency.

2. Nuclear contribution to the zero-field relaxation

The exponential relaxation observed in ZF-μSR, including the finite relaxation already present above T_c, is striking and reproducible between different samples. Its suppression by modest longitudinal fields indicates that the underlying local fields are predominantly static or quasistatic. One possible source of static local fields is the nuclear moments.

Oxygen has no nuclear moment, apart from the 0.04% natural abundance of ^{17}O, whereas ^{87}Sr, ^{99}Ru, and ^{101}Ru have finite nuclear moments and natural abundances of approximately 7%, 13%, and 17%, respectively. The remaining isotopes have $I = 0$. This corresponds to a relatively dilute background of nuclear spins. We simulated the relaxation expected from these nuclear moments using a Monte Carlo method. The result, shown in Fig. S12 of the Supplementary Information, is much closer to a Gaussian-like relaxation than to the experimentally observed exponential form. In addition, its magnitude is too small to account for the measured relaxation. We therefore conclude that static nuclear moments alone cannot explain the observed exponential character of the ZF-μSR relaxation.

B. Possible sources of the low-temperature relaxation

Our data impose several constraints on the possible microscopic origin of the relaxation. The relevant mechanism must already be present in the normal state, must produce similar temperature dependences in ZF-μSR and in TF-μSR at 80 mT, must lead to a smaller relaxation amplitude in TF than in ZF, must be nearly static at low temperatures, and must account for the exponential rather than Gaussian form of the ZF relaxation. We therefore consider below several possible sources of the low-temperature relaxation in light of these constraints.

The scenarios considered below include dilute or defect-related magnetism associated with Sr_2RuO_4 itself, surface-related altermagnetism, macroscopic or microscopic impurity phases, and effects associated with the implanted muon, such as trapping, hopping, or diffusion.

1. Dilute magnetic moments or defect-related magnetism in Sr_2RuO_4

Since the simulated nuclear contribution is both too weak and closer to a Gaussian-like relaxation, we next consider a dilute distribution of electronic moments. For a static dilute distribution of randomly located moments, the relaxation may approach a Lorentzian Kubo–Toyabe form [46, 47], $G(t) = \frac{1}{3} + \frac{2}{3}(1 - at)\exp(-at)$, which is approximately exponential at early times, $G(t) \simeq \exp(-\Lambda t)$, with $\Lambda = 4a/3$; see the Supplementary Information for details. Taking $\Lambda \simeq 0.04\ \mu s^{-1}$ and moments of order 1 μ_B gives an estimated magnetic-site concentration $c \simeq 800$ ppm. Such dilute electronic moments could be associated with Ru-site vacancies, antisite defects, oxygen defects, or local strain fields that polarize nearby Ru orbitals. In this picture, a nominally nonmagnetic structural defect could generate a spatially extended Ru spin polarization.

The LF-μSR data provide the most direct constraint on this interpretation. As shown in Fig. 6, the relaxation is rapidly suppressed by small longitudinal fields at 2 K. A weak longitudinal field can decouple the muon spins from a static or slowly fluctuating distribution of dilute local fields [36, 37]. The observed LF decoupling therefore indicates that, once the low-temperature relaxation has developed, the fields sensed by the muons are predominantly static or quasistatic on the μSR time scale.

The comparison between the ZF and TF relaxation amplitudes gives an additional consistency check. In ZF, the muon polarization is relaxed by the full distribution of randomly oriented local fields. In a transverse applied field, the external field defines the dominant precession axis and partially averages or decouples the effect of the local-field components perpendicular to it. For a static or quasistatic dilute field distribution, the TF relaxation is therefore expected to be reduced compared with the ZF relaxation, while retaining a similar temperature dependence if both measurements probe the same underlying magnetic source [37]. The observation that $\Delta\Lambda^{\mathrm{TF,80mT}}$ is smaller than $\Delta\Lambda^{\mathrm{ZF}}$, but both $\Lambda^{\mathrm{ZF}}(T)$ and $\Lambda^{\mathrm{TF,80mT}}(T)$ follow a comparable temperature dependence, is consistent with this expectation.

The field dependence of the normal-state TF relaxation provides further information on the origin of the relevant relaxation channel. Figure 4 indicates that $\Lambda^{\mathrm{TF}}(T)$ starts to increase already above $T_c(H)$, as part of the same relaxation channel that is also present at 80 mT. As shown in Fig. 5, the characteristic temperature scale associated with the increase of $\Lambda^{\mathrm{TF}}(T)$ appears to shift to higher temperatures with increasing applied field. Since the high-field measurements were performed above $H_{c2}^{\|c}(0)$, this shift is not related to the superconducting mixed state. A possible interpretation is that the applied field polarizes dilute moments, magnetic clusters, or defect-related magnetic regions, thereby modifying the quasistatic local-field distribution sensed by the muons. In this sense, the field dependence may reflect a field-tuned crossover of a normal-state magnetic background rather than a superconducting transition. Thus, within the scenarios discussed in this subsection, the field dependence of T_Λ should not be interpreted as evidence for a purely fast-fluctuating Redfield-type process, but rather as a possible field tuning of a static or quasistatic local-field distribution.

This explanation is related, but not identical, to defect-induced TRSB models [19]. In such models, a primarily single-component superconducting state can acquire local complex components near strain fields or dislocations, generating spontaneous fields in an inhomogeneous man-

ner. The persistence of the 80 mT response when bulk superconductivity is suppressed shows that such a superconducting mechanism cannot account for the entire relaxation. Nevertheless, local defects remain a plausible common ingredient in both superconducting and non-superconducting interpretations.

2. Surface-related altermagnetism

Recent theoretical works have proposed altermagnetism as a possible origin of weak time-reversal-symmetry-breaking magnetism in Sr_2RuO_4, especially in connection with local symmetry lowering caused by surface reconstruction and rotations of the RuO_6 octahedra [48, 49]. Such a distortion may stabilize a compensated magnetic state with no, or only very small, net magnetization, while still producing weak static or quasistatic local fields detectable by μSR.

These theoretical proposals are closely connected to the earlier low-energy (LE) μSR observation of weak static surface magnetism in Sr_2RuO_4 [50]. This is relevant here because the LE-μSR response shows several qualitative similarities to the additional exponential relaxation observed in our measurements: it is seen in the normal state, appears in TF-μSR, and LF-μSR indicates that the associated local fields are static or quasistatic.

A further important point is the depth dependence of the LE-μSR signal. The strongest increase of the relaxation rate was observed for muons stopping within approximately 10–20 nm from the surface, with an onset temperature of $\sim$ 50–75 K. At larger implantation depths, such as about 70 nm, the effect becomes weaker and appears only below approximately 25 K [50]. This suggests that the characteristic temperature scale detected by μSR may depend on the muon stopping depth. The so-called "surface" muons used in the present experiment have an energy of $\simeq$ 4 MeV and therefore stop much deeper in the sample, at typical depths of order 0.1–0.2 mm (see, e.g., Fig. 2 in Ref. 51).

A connection between these observations remains speculative. The present data do not provide direct evidence for altermagnetism, and the large difference between LE-μSR and conventional μSR stopping depths excludes a simple one-to-one correspondence. Such a connection would require that surface-related magnetism, or a related defect- or strain-induced magnetic state, gives rise to weak static local fields also within the bulk, for example in the vicinity of stacking faults, dislocations, structural domains, or other locally strained regions. In this context, altermagnetism may provide a possible microscopic route to the weak static magnetic background observed in Sr_2RuO_4.

3. Role of macroscopic and microscopic impurity phases

A possible extrinsic source of local magnetic fields in Sr_2RuO_4 is the presence of secondary phases from the Sr–Ru–O phase diagram. Depending on small deviations from the ideal growth conditions, crystals may contain traces of Ru lamellae, $SrRuO_3$ (the 113 phase), $Sr_3Ru_2O_7$ (the 327 phase), or other higher-order Ruddlesden–Popper ruthenates. These phases can occur either as macroscopic inclusions or, more subtly, as microscopic intergrowths or stacking-fault defects within the Sr_2RuO_4 matrix.

Ru-metal inclusions represent a well-known example of such secondary phases. They are known to enhance the local superconducting transition temperature to $T_c \simeq 3$ K and the upper critical field to $H_{c2}^{\parallel c}(0) \simeq 1$ T [52]. The ac-susceptibility results shown in Fig. S3 of the Supplementary Information demonstrate that the samples used in this study contain only a negligible amount of such Ru inclusions. Ru-metal inclusions are therefore unlikely to be responsible for the observed low-temperature exponential μSR relaxation.

We next consider ruthenate impurity phases related to the 113 and 327 structures. The 113 phase is ferromagnetic, while the 327 phase exhibits strongly enhanced paramagnetic susceptibility. Their presence can therefore be tested by dc-magnetization measurements, providing an independent way to assess whether macroscopic $SrRuO_3$ or $Sr_3Ru_2O_7$ impurity phases could be responsible for the observed exponential μSR relaxation.

In addition to macroscopic impurity phases, 113- or 327-like structural fragments may also occur as microscopic intergrowths or stacking-fault defects within the Sr_2RuO_4 matrix. In this case, local deviations from the ideal 214 stacking sequence can produce fragments resembling the 113, 327, or other related Ruddlesden–Popper phases. The volume fraction of such microscopic intergrowths is expected to be much smaller than that of resolvable macroscopic impurity phases, and they may therefore be difficult to detect by standard bulk characterization. Nevertheless, if they are magnetic or strongly polarizable, they could contribute to an inhomogeneous static or quasistatic local-field distribution sensed by the muons.

To test the role of macroscopic 113 and 327 impurity phases, we performed dc-susceptibility measurements on pieces cut from the same growth rods as the μSR samples. The results, shown in Fig. S4 of the Supplementary Information, reveal sample-dependent low-level impurity contributions. In particular, a magnetic onset near 160 K is consistent with traces of the 113 phase, while a feature around 20 K is characteristic of the 327 phase.

The relative magnitude of these impurity signatures differs substantially between the samples. For example, sample A exhibits comparatively strong contributions associated with the 113 and 327 phases, corresponding to estimated impurity levels of approximately 600 ppm and 1.3%, respectively. By contrast, sample C shows the

weakest signatures of both 113 and 327 impurity phases. This variation does not correlate with the μSR results: the low-temperature increase of the exponential relaxation rate Λ is observed in all samples and displays a broadly similar temperature dependence despite the substantially different impurity signatures inferred from the magnetization measurements. Moreover, the relaxation enhancement $\Delta\Lambda$ does not scale with the magnitude of the macroscopic impurity signatures. In particular, although sample C shows only weak 113 and 327 contributions in dc magnetization, its low-temperature increase of Λ is comparable to, or even larger than, that observed in samples with substantially stronger impurity signatures, such as samples A and B. We therefore conclude that macroscopic $SrRuO_3$ or $Sr_3Ru_2O_7$ impurity phases are unlikely to be the primary origin of the observed exponential μSR relaxation.

This conclusion does not completely exclude a contribution from microscopic intergrowths, stacking faults, or other local structural defects that are not resolved as macroscopic impurity phases. However, such defects would represent a dilute, spatially inhomogeneous source of static or quasistatic local fields, rather than a bulk impurity phase. They therefore fall within the broader class of defect-related magnetic backgrounds discussed above.

4. Muon-induced effects

Muon trapping, changes of stopping configuration, or local hopping among muon stopping sites can also produce a temperature-dependent exponential relaxation [37, 53–60]. The calculations discussed above indicate that long-range diffusion between sites associated with different apical oxygen atoms is negligible at the temperatures of our measurements. Local hopping or delocalization among the four symmetry-equivalent positions around a given apical oxygen, however, may still modify the local-field distribution sampled by the muon. Upon cooling, changes in the local muon state or trapping near defects could similarly lead to an increased relaxation rate.

This mechanism is relevant because the relaxation channel is already present above T_Λ and becomes enhanced on cooling, rather than appearing abruptly at T_c. The smooth onset, the presence of the effect in the normal state, and the LF decoupling are compatible with this class of explanations, provided that the low-temperature muon state samples a predominantly static or quasistatic local-field distribution. In this case, muon trapping or a change of site would not itself constitute a fast dynamic relaxation mechanism, but would instead modify the static local fields sampled by the muon. Hopping or delocalization among symmetry-equivalent sites near the apical oxygen could similarly modify the coupling of the muon to local nuclear moments, electric-field gradients, or weak electronic moments. In addition, motion of the muon around the charged oxygen could, in principle, generate an effective magnetic field at the muon site and modify its response to an applied field. Whether such motion can remain sufficiently slow or quasistatic at low temperature, and whether it can account for the observed field dependence, remain open and highly speculative questions.

This scenario should be tested further by extending the temperature range above 2 K and by comparing samples with different defect concentrations, for example after controlled electron or ion irradiation. If muon trapping, changes in the local stopping configuration, or local hopping are involved, the characteristic temperature scale of the relaxation should depend on the local defect environment and possibly on the muon stopping configuration.

C. Consequences for TRSB in Sr_2RuO_4

Our ZF-μSR data are fully consistent with the previously published results on Sr_2RuO_4. They confirm that the low-temperature increase of the ZF exponential relaxation rate, appearing at or below T_c, is a robust and reproducible experimental observation. This anomaly has been reported over nearly three decades, on different samples and using different instruments and facilities [6, 7, 16, 22, 23, 28–30]. The new aspect of the present study is that a closely related exponential relaxation channel is also detected when bulk superconductivity is suppressed by an applied field above $H_{c2}^{\|c}(0)$. This demonstrates that the total relaxation contains a normal-state contribution, which must be accounted for before assigning the ZF relaxation increase uniquely to superconducting TRSB.

An earlier hydrostatic-pressure study found that T_Λ and T_c are suppressed together [16], which naturally suggested a connection between the additional relaxation and superconductivity. This observation remains important, but it does not by itself establish that the relaxation is caused directly by a homogeneous TRSB superconducting order parameter. Experiments under uniaxial stress also indicate a slight suppression of T_Λ, at least initially [22, 23]. If pressure generally reduces the characteristic temperature scale of the relaxation channel, the apparent tracking of T_Λ and T_c under hydrostatic pressure may reflect two pressure-dependent quantities that vary in parallel. Alternatively, the weak static magnetic background may be coupled to the same low-energy electronic, magnetic, or lattice degrees of freedom that are affected by pressure and are relevant for superconductivity. This interpretation remains speculative, but it removes an apparent contradiction between the pressure results and the present high-field TF-μSR data.

This broader interpretation is also consistent with thermodynamic studies under uniaxial pressure and strain, which have found no evidence for an additional bulk transition below T_c or for the transition splitting expected for a homogeneous two-component TRSB superconducting state [24–26]. Such an absence is difficult to recon-

cile with a homogeneous two-component superconducting state in which a separate TRSB transition occurs below T_c, since such a transition would generally be expected to produce a thermodynamic anomaly. Our results offer a possible explanation for this discrepancy: the low-temperature μSR relaxation previously attributed to spontaneous superconducting fields may be due, at least in part, to a process that is also present in the normal state. In this case, the onset temperature T_Λ extracted from μSR need not correspond to a bulk superconducting TRSB transition.

The TF data below $H_{c2}^{\|c}(0)$ further support this interpretation. In the superconducting mixed state, the exponential relaxation contains both the normal-state channel and an additional flux-line-lattice-related contribution. In ZF, there is no vortex lattice, but a related normal-state exponential relaxation channel may still be present and can mimic an onset of spontaneous internal fields. Consequently, any claim of superconducting TRSB from μSR in Sr_2RuO_4 should demonstrate that the enhanced relaxation is not caused by a normal-state contribution, for example by determining the relaxation channel after superconductivity is suppressed.

V. SUMMARY

We studied four Sr_2RuO_4 single crystals from different growth batches, focusing on the low-temperature increase of the exponential relaxation rate Λ, which in previous ZF-μSR studies was assigned to the onset of TRSB superconductivity. Three crystals with superconducting transition temperatures T_c=1.51, 1.48, and 1.40 K were studied using ZF-, TF-, and LF-μSR. In addition, ZF-μSR data for a fourth crystal with T_c=1.35 K are discussed in the Supplementary Information. In all four ZF data sets, Λ increases below a characteristic temperature T_Λ that is separated from the bulk superconducting transition temperature. This behavior follows the trend observed in several other ZF-μSR studies of unstrained Sr_2RuO_4, where T_Λ is not universally locked to T_c.

DFT calculations confirm that the muon stopping site is located near an apical oxygen of a RuO_6 octahedron, with possible delocalization over four symmetry-equivalent positions. The relaxation expected from the naturally abundant nuclear moments of Sr and Ru was estimated by Monte Carlo simulations. The calculated nuclear contribution is closer to a Gaussian-like relaxation and is too weak to account for the experimentally observed exponential relaxation, indicating that static nuclear moments alone cannot explain the data.

A central result is that a quantitatively similar relaxation channel is observed in TF-μSR at 80 mT. Since this field exceeds $H_{c2}^{\|c}(0)$ for the present crystals, the samples are in the normal state and the relaxation cannot originate from the superconducting state itself. The temperature dependence and onset scale are close to those observed in ZF, while the amplitude of the relaxation enhancement is smaller in TF than in ZF. This reduction is consistent with expectations for a static or quasistatic dilute local-field distribution in an applied transverse field.

Measurements below $H_{c2}^{\|c}(0)$ reveal an additional superconducting mixed-state contribution potentially associated with the flux-line lattice. Thus, the TF relaxation below $H_{c2}^{\|c}(0)$ should be viewed as a superposition of the normal-state exponential channel and a superconducting contribution. Measurements above $H_{c2}^{\|c}(0)$ show that the characteristic temperature scale of the normal-state relaxation is field dependent, further excluding a simple temperature-independent nuclear dipolar background. In particular, the apparent T_Λ scale tends to increase with increasing transverse field above $H_{c2}^{\|c}(0)$, suggesting that this normal-state relaxation channel is field tunable. This behavior may reflect field-induced polarization or gradual freezing of dilute defect-related moments, rather than a temperature-independent background.

LF-μSR measurements show that the relaxation is strongly suppressed by small longitudinal fields, indicating that the underlying local fields are static or quasistatic on the μSR time scale. In the superconducting state, LF measurements must be interpreted with caution because partial diamagnetism, vortex penetration, and geometrical barriers in finite rectangular crystals can generate nonuniform internal fields and local components perpendicular to the nominal LF direction.

Taken together, the data show that the exponential relaxation detected in ZF-μSR experiments on Sr_2RuO_4 cannot be assigned uniquely to spontaneous fields of superconducting origin. The most natural explanations are dilute magnetic moments or defect-related magnetism. The muon stopping-site results and the nuclear-spin simulation support this conclusion by showing that the conventional static nuclear contribution is insufficient, while the observed exponential form is more naturally compatible with dilute or spatially inhomogeneous sources of local fields. A gradual freezing or slowing down of dilute defect-related moments may contribute to the onset of the relaxation, but the LF data indicate that the low-temperature state is predominantly static or quasistatic.

ACKNOWLEDGMENTS

This work is based on experiments performed at the Swiss Muon Source SμS, Paul Scherrer Institute, Villigen, Switzerland. The authors acknowledge P. Dalmas de Réotier, M. Sigrist, J. Sonier, and A. Mackenzie for helpful discussions and A. Ikeda and H. Matsuki for their contributions in characterizing some of the samples. The work of N.K. was supported by JSPS KAKENHI (No. JP21H01033, No. JP22K19093, and JP24K01461). B.M.H. and S.J.B. acknowledge support from UK Research and Innovation (UKRI) under the UK Government's Horizon Europe funding guarantee [Grant No. EP/X025861/1].

AUTHOR CONTRIBUTIONS

R.K. and Y.M. conceived and coordinated the study and conducted the μSR experiments. R.K. analyzed the data and wrote the manuscript with input from all authors. T.J.H., J.A.K., T.S., and H.L. contributed to the μSR experiments. J.S.B., T.J., N.K., and Y.M. contributed to sample preparation and characterization. B.M.H. and S.J.B. performed the muon-site and related computational calculations and analyzed the results. R.K., T.J.H., J.A.K., M.L., T.S., J.S.B., V.G., T.J., N.K., H.-H.K., S.P., B.M.H., S.J.B., H.L., and Y.M. discussed the results and reviewed the manuscript. All authors approved the final version.

ETHICS DECLARATION

Not applicable.

DATA AVAILABILITY

The data supporting the findings of this study are available within the Article and its Supplementary Information. Additional data, including the underlying experimental data, are available from the corresponding author upon reasonable request.

COMPETING INTERESTS

The authors declare no competing interests.

[1] Y. Maeno, H. Hashimoto, K. Yoshida, S. Nishizaki, T. Fujita, J. G. Bednorz, and F. Lichtenberg, *Superconductivity in a layered perovskite without copper*, Nature (London) **372**, 532 (1994). https://doi.org/10.1038/372532a0

[2] A. P. Mackenzie and Y. Maeno, *The superconductivity of Sr_2RuO_4 and the physics of spin-triplet pairing*, Rev. Mod. Phys. **75**, 657 (2003). https://doi.org/10.1103/RevModPhys.75.657

[3] Y. Maeno, S. Yonezawa, and A. Ramires, *Still mystery after all these years – Unconventional superconductivity of Sr_2RuO_4*, J. Phys. Soc. Jpn. **93**, 062001 (2024). https://doi.org/10.7566/JPSJ.93.062001

[4] Y. Maeno, A. Ikeda, and G. Mattoni, *Thirty years of puzzling superconductivity in Sr_2RuO_4*, Nat. Phys. **20**, 1712 (2024). https://doi.org/10.1038/s41567-024-02656-0

[5] K. Ishida, H. Mukuda, Y. Kitaoka, K. Asayama, Z. Q. Mao, Y. Mori, and Y. Maeno, *Spin-triplet superconductivity in Sr_2RuO_4 identified by ^{17}O Knight shift*, Nature **396**, 658 (1998). https://doi.org/10.1038/25315

[6] G. M. Luke, Y. Fudamoto, K. M. Kojima, M. I. Larkin, J. Merrin, B. Nachumi, Y. J. Uemura, Y. Maeno, Z. Q. Mao, Y. Mori, H. Nakamura, and M. Sigrist, *Time-reversal symmetry-breaking superconductivity in Sr_2RuO_4*, Nature (London) **394**, 558 (1998). https://doi.org/10.1038/29038

[7] G. M. Luke, Y. Fudamoto, K. M. Kojima, M. I. Larkin, B. Nachumi, Y. J. Uemura, J. E. Sonier, Y. Maeno, Z. Q. Mao, Y. Mori, and D. F. Agterberg, *Unconventional superconductivity in Sr_2RuO_4*, Physica B **289-290**, 373 (2000). https://doi.org/10.1016/S0921-4526(00)00414-2

[8] J. Xia, Y. Maeno, P. T. Beyersdorf, M. M. Fejer, and A. Kapitulnik, *High Resolution Polar Kerr Effect Measurements of Sr_2RuO_4: Evidence for Broken Time-Reversal Symmetry in the Superconducting State*, Phys. Rev. Lett. **97**, 167002 (2006). https://doi.org/10.1103/PhysRevLett.97.167002

[9] F. Kidwingira, J. D. Strand, D. J. Van Harlingen, and Y. Maeno, *Dynamical Superconducting Order Parameter Domains in Sr_2RuO_4*, Science **314**, 1267 (2006). https://doi.org/10.1126/science.1133239

[10] M. S. Anwar, T. Nakamura, S. Yonezawa, M. Yakabe, R. Ishiguro, H. Takayanagi, and Y. Maeno, *Anomalous switching in Nb/Ru/Sr_2RuO_4 topological junctions by chiral domain wall motion*, Sci. Rep. **3**, 2480 (2013). https://doi.org/10.1038/srep02480

[11] A. Pustogow, Y. K. Luo, A. Chronister, Y.-S. Su, D. A. Sokolov, F. Jerzembeck, A. P. Mackenzie, C. W. Hicks, N. Kikugawa, S. Raghu, E. D. Bauer, and S. E. Brown, *Constraints on the superconducting order parameter in Sr_2RuO_4 from oxygen-17 nuclear magnetic resonance*, Nature (London) **574**, 72 (2019). https://doi.org/10.1038/s41586-019-1596-2

[12] K. Ishida, M. Manago, K. Kinjo, and Y. Maeno, *Reduction of the ^{17}O Knight Shift in the Superconducting State and the Heat-up Effect by NMR Pulses on Sr_2RuO_4*, J. Phys. Soc. Jpn. **89**, 034712 (2020). https://doi.org/10.7566/JPSJ.89.034712

[13] A. Chronister, A. Pustogow, N. Kikugawa, D. A. Sokolov, F. Jerzembeck, C. W. Hicks, A. P. Mackenzie, E. D. Bauer, and S. E. Brown, *Evidence for even parity unconventional superconductivity in Sr_2RuO_4*, Proc. Natl. Acad. Sci. USA **118**, e2025313118 (2021). https://doi.org/10.1073/pnas.2025313118

[14] A. N. Petsch, M. Zhu, M. Enderle, Z. Q. Mao, Y. Maeno, I. I. Mazin, and S. M. Hayden, *Reduction of the Spin Susceptibility in the Superconducting State of Sr_2RuO_4 Observed by Polarized Neutron Scattering*, Phys. Rev. Lett. **125**, 217004 (2020). https://doi.org/10.1103/PhysRevLett.125.217004

[15] H. Matsuki, R. Khasanov, J. A. Krieger, T. J. Hicken, K. Yuchi, J. S. Bobowski, G. Mattoni, A. Ikeda, R. Okuma, H. Luetkens, and Y. Maeno, *Muon Knight Shift as a Pre-*

cise Probe of the Superconducting Symmetry of Sr_2RuO_4, Phys. Rev. Lett. **136**, 066001 (2026). https://doi.org/10.1103/sgcz-9rc7

[16] V. Grinenko, D. Das, R. Gupta, B. Zinkl, N. Kikugawa, Y. Maeno, C. W. Hicks, H.-H. Klauss, M. Sigrist, and R. Khasanov, *Unsplit superconducting and time reversal symmetry breaking transitions in Sr_2RuO_4 under hydrostatic pressure and disorder*, Nat. Commun. **12**, 3920 (2021). https://doi.org/10.1038/s41467-021-24176-8

[17] A. T. Rømer, T. A. Maier, A. Kreisel, P. J. Hirschfeld, and B. M. Andersen, *Leading superconducting instabilities in three-dimensional models for Sr_2RuO_4*, Phys. Rev. Research **4**, 033011 (2022). https://doi.org/10.1103/PhysRevResearch.4.033011

[18] M. Sigrist and K. Ueda, *Phenomenological theory of unconventional superconductivity*, Rev. Mod. Phys. **63**, 239 (1991). https://doi.org/10.1103/RevModPhys.63.239

[19] R. Willa, M. Hecker, R. M. Fernandes, and J. Schmalian, *Inhomogeneous time-reversal symmetry breaking in Sr_2RuO_4*, Phys. Rev. B **104**, 024511 (2021). https://doi.org/10.1103/PhysRevB.104.024511

[20] S. Ghosh, A. Shekhter, F. Jerzembeck, N. Kikugawa, D. A. Sokolov, M. Brando, A. P. Mackenzie, C. W. Hicks, and B. J. Ramshaw, *Thermodynamic evidence for a two-component superconducting order parameter in Sr_2RuO_4*, Nat. Phys. **17**, 199 (2021). https://doi.org/10.1038/s41567-020-1032-4

[21] S. Benhabib, C. Lupien, I. Paul, L. Berges, M. Dion, M. Nardone, A. Zitouni, Z. Q. Mao, Y. Maeno, A. Georges, L. Taillefer, and C. Proust, *Ultrasound evidence for a two-component superconducting order parameter in Sr_2RuO_4*, Nat. Phys. **17**, 194 (2021). https://doi.org/10.1038/s41567-020-1033-3

[22] V. Grinenko, S. Ghosh, R. Sarkar, J.-C. Orain, A. Nikitin, M. Elender, D. Das, Z. Guguchia, F. Brueckner, M. E. Barber, J. Park, N. Kikugawa, D. A. Sokolov, J. Bobowski, T. Miyoshi, Y. Maeno, A. P. Mackenzie, H. Luetkens, C. W. Hicks, and H.-H. Klauss, *Split superconducting and time-reversal symmetry-breaking transitions in Sr_2RuO_4 under stress*, Nat. Phys. **17**, 748 (2021). https://doi.org/10.1038/s41567-021-01182-7

[23] V. Grinenko, R. Sarkar, S. Ghosh, D. Das, Z. Guguchia, H. Luetkens, I. Shipulin, A. Ramires, N. Kikugawa, Y. Maeno, K. Ishida, C. W. Hicks, and H.-H. Klauss, *Uniaxial stress-controlled time-reversal symmetry breaking in Sr_2RuO_4*, Phys. Rev. B **107**, 024508 (2023). https://doi.org/10.1103/PhysRevB.107.024508

[24] Y.-S. Li, N. Kikugawa, D. A. Sokolov, F. Jerzembeck, A. S. Gibbs, Y. Maeno, C. W. Hicks, J. Schmalian, M. Nicklas, and A. P. Mackenzie, *High-sensitivity heat-capacity measurements on Sr_2RuO_4 under uniaxial pressure*, Proc. Natl. Acad. Sci. USA **118**, e2020492118 (2021). https://doi.org/10.1073/pnas.2020492118

[25] Y.-S. Li, M. Garst, J. Schmalian, S. Ghosh, N. Kikugawa, D. A. Sokolov, C. W. Hicks, F. Jerzembeck, M. S. Ikeda, Z. Hu, B. J. Ramshaw, A. W. Rost, M. Nicklas, and A. P. Mackenzie, *Elastocaloric determination of the phase diagram of Sr_2RuO_4*, Nature **607**, 276–280 (2022). https://doi.org/10.1038/s41586-022-04820-z

[26] F. Jerzembeck, Y.-S. Li, G. Palle, Z. Hu, M. Biderang, N. Kikugawa, D. A. Sokolov, S. Ghosh, B. J. Ramshaw, T. Scaffidi, M. Nicklas, J. Schmalian, A. P. Mackenzie, and C. W. Hicks, *T_c and the elastocaloric effect of Sr_2RuO_4 under $\langle 110 \rangle$ uniaxial stress: No indications of transition splitting*, Phys. Rev. B **110**, 064514 (2024). https://doi.org/10.1103/PhysRevB.110.064514

[27] T. Shiroka, R. Fittipaldi, M. Cuoco, R. De Renzi, Y. Maeno, R. J. Lycett, S. Ramos, E. M. Forgan, C. Baines, A. W. Rost, V. Granata, and A. Vecchione, *μSR studies of the superconducting state of Sr_2RuO_4*, Phys. Rev. B **85**, 134527 (2012). https://doi.org/10.1103/PhysRevB.85.134527

[28] W. Higemoto, A. Koda, R. Kadono, Y. Yoshida, and Y. Onuki, *Investigation of Spontaneous Magnetic Field in Spin-Triplet Superconductor Sr_2RuO_4*, JPS Conf. Proc. **2**, 010202 (2014). https://doi.org/10.7566/JPSCP.2.010202

[29] R. Khasanov, A. Ramires, V. Grinenko, I. Shipulin, N. Kikugawa, D. A. Sokolov, J. A. Krieger, T. J. Hicken, Y. Maeno, H. Luetkens, and Z. Guguchia, *In-plane magnetic penetration depth in Sr_2RuO_4: Muon-spin rotation and relaxation study*, Phys. Rev. Lett. **131**, 236001 (2023). https://doi.org/10.1103/PhysRevLett.131.236001

[30] Y. Li, R. Khasanov, S. P. Cottrell, N. Kikugawa, Y. Maeno, B. Zhao, J. Ma, and V. Grinenko, *Origins of spontaneous magnetic fields in Sr_2RuO_4*, arXiv:2512.24585 (2025). https://doi.org/10.48550/arXiv.2512.24585

[31] J. S. Bobowski, N. Kikugawa, T. Miyoshi, H. Suwa, H.-s. Xu, S. Yonezawa, D. A. Sokolov, A. P. Mackenzie, and Y. Maeno, *Improved single-crystal growth of Sr_2RuO_4*, Condensed Matter **4**, 6 (2019). https://doi.org/10.3390/condmat4010006

[32] A. Suter and B. M. Wojek, *Musrfit: A free platform-independent framework for μSR data analysis*, Phys. Procedia **30**, 69 (2012). https://doi.org/10.1016/j.phpro.2012.04.042

[33] T. M. Riseman, P. G. Kealey, E. M. Forgan, A. P. Mackenzie, L. M. Galvin, A. W. Tyler, S. L. Lee, C. Ager, D. McK. Paul, C. M. Aegerter, R. Cubitt, Z. Q. Mao, T. Akima, and Y. Maeno, *Observation of a square flux-line lattice in the unconventional superconductor Sr_2RuO_4*, Nature (London) **396**, 242 (1998). https://doi.org/10.1038/24335

[34] S. Kittaka, T. Nakamura, Y. Aono, S. Yonezawa, K. Ishida, and Y. Maeno, *Angular dependence of the upper critical field of Sr_2RuO_4*, Phys. Rev. B **80**, 174514 (2009). https://doi.org/10.1103/PhysRevB.80.174514

[35] N. R. Werthamer, E. Helfand, and P. C. Hohenberg, *Temperature and purity dependence of the superconducting critical field, H_{c2}. III. Electron spin and spin-orbit effects*, Phys. Rev. **147**, 295 (1966). https://doi.org/10.1103/PhysRev.147.295

[36] R. S. Hayano, Y. J. Uemura, J. Imazato, N. Nishida, T. Yamazaki, and R. Kubo, *Zero- and low-field spin relaxation studied by positive muons*, Phys. Rev. B **20**, 850 (1979). https://doi.org/10.1103/PhysRevB.20.850

[37] A. Yaouanc and P. Dalmas de Réotier, *Muon Spin Rotation, Relaxation, and Resonance: Applications to Condensed Matter* (Oxford University Press, Oxford, 2011).

[38] E. H. Brandt, *Superconductors of finite thickness in a perpendicular magnetic field: Strips and slabs*, Phys. Rev. B **54**, 4246 (1996).

https://doi.org/10.1103/PhysRevB.54.4246
[39] E. Zeldov, A. I. Larkin, V. B. Geshkenbein, M. Konczykowski, D. Majer, B. Khaykovich, V. M. Vinokur, and H. Shtrikman, *Geometrical barriers in high-temperature superconductors*, Phys. Rev. Lett. **73**, 1428 (1994). https://doi.org/10.1103/PhysRevLett.73.1428
[40] E. H. Brandt, *Irreversible magnetization of pin-free type-II superconductors*, Phys. Rev. B **60**, 11939 (1999). https://doi.org/10.1103/PhysRevB.60.11939
[41] E. H. Brandt, *Superconductors in realistic geometries: Geometric edge barrier versus pinning*, Physica C **332**, 99–107 (2000). https://doi.org/10.1016/S0921-4534(99)00651-6
[42] E. H. Brandt, G. P. Mikitik, and E. Zeldov, *Two regimes of vortex penetration into platelet-shaped type-II superconductors*, J. Exp. Theor. Phys. **117**, 439 (2013). https://doi.org/10.1134/S1063776113110010
[43] S. J. Clark, M. D. Segall, C. J. Pickard, P. J. Hasnip, M. I. J. Probert, K. Refson, and M. C. Payne, *First principles methods using CASTEP*, Z. Kristallogr. Cryst. Mater. **220**, 567–570 (2005). https://doi.org/10.1524/zkri.220.5.567.65075
[44] B. M. Huddart, A. Hernández-Melián, T. J. Hicken, M. Gomilšek, Z. Hawkhead, S. J. Clark, F. L. Pratt, and T. Lancaster, *MuFinder: A program to determine and analyse muon stopping sites*, Comput. Phys. Commun. **280**, 108488 (2022). https://doi.org/10.1016/j.cpc.2022.108488
[45] B. M. Huddart, I. J. Onuorah, M. M. Isah, P. Bonfà, S. J. Blundell, S. J. Clark, R. De Renzi, and T. Lancaster, *Intrinsic nature of spontaneous magnetic fields in superconductors with time-reversal symmetry breaking*, Phys. Rev. Lett. **127**, 237002 (2021). https://doi.org/10.1103/PhysRevLett.127.237002
[46] A. T. Fiory, *Muon-spin relaxation in systems of dilute dipolar impurities: Numerical treatment of fluctuations*, Hyperfine Interact. **8**, 777–780 (1981). https://doi.org/10.1007/BF01037561
[47] G. A. Gist and S. A. Dodds, *Zero-field muon-spin-resonance linewidths in dilute magnetic alloys*, Phys. Rev. B **30**, 2340–2344 (1984). https://doi.org/10.1103/PhysRevB.30.2340
[48] C. Autieri, G. Cuono, D. Chakraborty, P. Gentile, and A. M. Black-Schaffer, *Conditions for orbital-selective altermagnetism in Sr_2RuO_4: Tight-binding model, similarities with cuprates, and implications for superconductivity*, Phys. Rev. B **112**, 014412 (2025). https://doi.org/10.1103/ssxp-gz91
[49] A. Ramires, *From pure to mixed: Altermagnets as intrinsic symmetry-breaking indicators*, arXiv:2502.19162 (2025). https://doi.org/10.48550/arXiv.2502.19162
[50] R. Fittipaldi, R. Hartmann, M. T. Mercaldo, S. Komori, A. Bjørlig, W. Kyung, Y. Yasui, T. Miyoshi, L. A. B. Olde Olthof, C. M. Palomares Garcia, V. Granata, I. Keren, W. Higemoto, A. Suter, T. Prokscha, A. Romano, C. Noce, C. Kim, Y. Maeno, E. Scheer, B. Kalisky, J. W. A. Robinson, M. Cuoco, Z. Salman, A. Vecchione, and A. Di Bernardo, *Unveiling unconventional magnetism at the surface of Sr_2RuO_4*, Nat. Commun. **12**, 5792 (2021). https://doi.org/10.1038/s41467-021-26020-5
[51] R. Khasanov, *Perspective on muon-spin rotation/relaxation under hydrostatic pressure*, J. Appl. Phys. **132**, 190903 (2022). https://doi.org/10.1063/5.0119840
[52] Y. Maeno, T. Ando, Y. Mori, E. Ohmichi, S. Ikeda, S. Nishizaki, and S. Nakatsuji, *Enhancement of superconductivity of Sr_2RuO_4 to 3 K by embedded metallic microdomains*, Phys. Rev. Lett. **81**, 3765 (1998). https://doi.org/10.1103/PhysRevLett.81.3765
[53] O. Hartmann, E. Karlsson, S. W. Harris, R. Wäppling, and T. O. Niinikoski, *Experimental support for the Kondo theory for light particle tunneling in metals*, Phys. Lett. A **142**, 504–508 (1989). https://doi.org/10.1016/0375-9601(89)90523-9
[54] R. Kadono, R. F. Kiefl, S. R. Kreitzman, Q. Li, T. Pfiz, T. M. Riseman, H. Zhou, R. Wäppling, S. W. Harris, O. Hartmann, and E. J. Ansaldo, *Quantum diffusion of the positive muon in the superconducting state of Al*, Hyperfine Interact. **64**, 737–741 (1991). https://doi.org/10.1007/BF02396211
[55] T. Pfiz, R. Kadono, R. F. Kiefl, S. R. Kreitzman, Q. Li, T. M. Riseman, H. Zhou, S. W. Harris, O. Hartmann, E. Karlsson, and E. J. Ansaldo, *Influence of superconductivity on quantum diffusion of the positive muon in aluminium*, J. Less-Common Met. **172–174**, 759–761 (1991). https://doi.org/10.1016/0022-5088(91)90200-N
[56] E. Karlsson, R. Wäppling, S. W. Lidström, O. Hartmann, R. Kadono, R. F. Kiefl, R. Hempelmann, and D. Richter, *Quantum diffusion and localization of positive muons in superconducting aluminum*, Phys. Rev. B **52**, 6417–6423 (1995). https://doi.org/10.1103/PhysRevB.52.6417
[57] M. Matsumoto and Y. Ohashi, *Quantum diffusion of muons interacting with superconducting electrons. I*, J. Phys. Soc. Jpn. **62**, 2088–2097 (1993). https://doi.org/10.1143/JPSJ.62.2088
[58] Y. Ohashi and M. Matsumoto, *Quantum diffusion of muons interacting with superconducting electrons. II*, J. Phys. Soc. Jpn. **62**, 3532–3538 (1993). https://doi.org/10.1143/JPSJ.62.3532
[59] S. J. Blundell, *Muon studies of superconductors*, Annu. Rev. Condens. Matter Phys. **16**, 367–385 (2025). https://doi.org/10.1146/annurev-conmatphys-032922-095149
[60] S. J. Blundell and T. Lancaster, *DFT+μ: Density functional theory for muon site determination*, Appl. Phys. Rev. **10**, 021316 (2023). https://doi.org/10.1063/5.0149080

Supplementary Files

This is a list of supplementary files associated with this preprint. Click to download.

- SupplementalMaterialSr2RuO4111026.pdf